JOURNAL OF GEOPHYSICAL RESEARCH, VOL. 98, NO. D10, PAGES 18,547–18,554, OCTOBER 20, 1993

Effect of Mount Pinatubo Aerosols on Total Ozone Measurements From Backscatter Ultraviolet (BUV) Experiments

P. K. BHARTIA, J. HERMAN, AND R. D. MCPETERS

Laboratory for Atmospheres, NASA Goddard Space Flight Center, Greenbelt, Maryland

O. TORRES

Hughes STX Corporation, Lanham, Maryland

Error introduced by Mount Pinatubo aerosols in total ozone derived by the backscatter ultraviolet (BUV) technique is described. BUV instruments include the total ozone mapping spectrometer (TOMS) instrument flying on Nimbus 7 and Meteor 3 satellites and solar backscattered ultraviolet (SBUV 2) instruments on NOAA weather satellites. Radiative transfer calculations show that except at very high solar zenith angles, errors in total ozone derived from the aerosol-contaminated radiances are less than 2% and vary both in magnitude and in sign with angles of observation. At solar zenith angles greater than 75°, total ozone values may be underestimated by as much as 10% if a large concentration of aerosols is present near the ozone density peak. In subsolar latitudes, error in total ozone derived from TOMS as a function of scan angle is very sensitive to the aerosol size distribution parameters. Aerosol parameters derived from these data agree well with in situ measurements.

1. INTRODUCTION

The eruption of Mount Pinatubo volcano in Philippines on June 15, 1991, injected large amounts of SO_2 high into the stratosphere that quickly converted into a dense sulfuric acid aerosol layer centered around 26 km [*Bluth et al.*, 1992; *McCormick and Veiga*, 1992]. Although the impact of this aerosol layer on stratospheric chemistry and dynamics is still under investigation, its impact on stratospheric sounding instruments, both ground and satellite based, has been considerable. Earlier studies of the effect of aerosols on BUV total ozone retrieval [*Dave*, 1978] have shown that the total ozone derived from the backscatter ultraviolet (BUV) technique is insensitive to tropospheric and lower stratospheric aerosols normally found in the Earth's atmosphere. However, the impact of a dense aerosol layer located near the ozone density peak has not been extensively studied.

Observations made by the solar backscattered ultraviolet (SBUV) instrument [*Bhartia et al.*, 1983] on Nimbus 7 satellite after the eruption of El Chichón volcano in April 1982 showed that the BUV radiances emanating from the Earth's atmosphere increased significantly after the eruption. The total ozone derived from these radiances, however, did not appear to have been affected significantly when compared to measurements from ground-based Dobson stations. However, after the eruption of Mount Pinatubo, daily ozone maps produced from the Nimbus 7/total ozone mapping instrument (TOMS) have shown a scan angle dependence in the derived ozone [*Schoeberl et al.*, 1993] in subsolar latitudes. (Similar artifacts have now been seen in the TOMS data taken after the eruption of El Chichón.)

Given the importance of accurate total ozone measurements for understanding the chemical and dynamical behavior of the stratosphere after major volcanic eruptions, we present here results from an extensive ongoing simulation study of the effect of aerosols on total ozone derived from BUV measurements. Results of this study are applicable to all operational BUV instruments, which includes the two TOMS instruments currently flying on NASA's Nimbus 7 and Russian Meteor 3 satellites, SBUV 2 instruments on NOAA 9 and 11 satellites, and two post-Pinatubo flights of the SSBUV instrument on the space shuttle.

Paper number 93JD01739.
0148-0227/93/93JD-01739$05.00

2. OPTICAL PROPERTIES OF SULFURIC ACID AEROSOLS IN UV

The BUV instruments use wavelengths in the Huggins band (312–331 nm) of the ozone absorption spectrum to derive total ozone. Wavelengths in the 340- to 380-nm region are used to estimate cloud and surface reflectivity effects on the BUV radiances. The effect of aerosols on these radiances is determined by the scattering cross section and phase function of the aerosols at the different wavelengths, which in turn depend upon the size distribution and refractive index of the aerosol particles.

Figure 1 shows the Mie scattering phase function at two extreme BUV total ozone wavelengths. The refractive indices (n) at the BUV total ozone wavelengths are extrapolated from the tables given by *Palmer and Williams* [1975], assuming 75% H_2SO_4 and 25% H_2O solution [*Hofmann and Rosen*, 1983]. The parameters of the assumed lognormal particle size distribution are the best fit values derived using the procedure discussed later in this paper. As is typical for aerosol scattering, 42% of the total scattered radiation goes in the forward direction within a narrow cone of 15° and about 38% goes in the backscattering direction between 150° and 180° scattering angles, with the remaining 20% going in other directions.

The oscillatory structure seen in the backscattering phase function is very sensitive to the wavelength (Figure 1) and assumed aerosol parameters. Figure 2 shows the sensitivity of the backscattering phase function to the index of refraction (n), the particle size distribution (r_0), and the width of

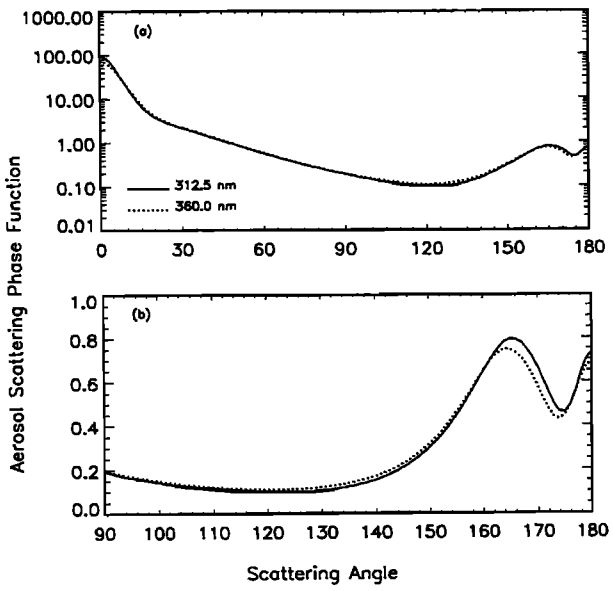

Fig. 1. Mie scattering phase function (normalized to $1/4\pi$), for (*a*) $\lambda = 312.5$ ($n = 1.470 + 0i$) and 360.0 nm ($n = 1.452 + 0i$), assuming lognormal particle size distribution, with $r_0 = 0.4$ μm and $\sigma = 1.5$. (*b*) The same phase function on an expanded linear scale in the backscattering direction only.

the size distribution, as defined by the standard deviation (σ) of the lognormal size distribution function. Under the right observing conditions the structures in the backscattering phase function can be directly observed in the TOMS total ozone data, providing us with a sensitive method to verify if realistic aerosol optical parameters have been selected for the radiative transfer model.

3. Effect of Stratospheric Aerosols on Backscatter Ultraviolet (BUV) Radiances

For single scattering the effect of aerosols on backscattered radiances is a function of the scattering angle Θ and is determined by the ratio of aerosol-scattering phase function to the Rayleigh-scattering phase function. For nadir-viewing instruments (SBUV, SBUV 2, and SSBUV), $\Theta = \pi - \theta_0$, where θ_0 is the solar zenith angle. For the scanning TOMS instrument the scattering angle is given by

$$\cos \Theta = \cos \theta_0 \cos \theta + \sin \theta_0 \sin \theta \cos \phi \qquad (1)$$

where θ is the satellite zenith angle and ϕ is the solar azimuth angle, defined in a Cartesian coordinate system with the Z axis pointing in the zenith direction at the center of the instantaneous field of view of the satellite and the X axis pointing toward the subsatellite point. Figure 3 shows contour maps of scattering angles for the Nimbus 7/TOMS instrument on two selected days in 1991. Since TOMS scans perpendicular to the plane of the orbit, scattering angles near 180° can occur only in the subsolar latitudes where the aerosol backscattering phase function is relatively large and has the characteristic oscillatory structure (Figure 4). TOMS data from these latitudes are particularly interesting for understanding the impact of aerosol on BUV radiances. As one moves away from the subsolar latitudes, the scattering angles get below 140°, where the aerosol backscattering phase function is small and is weakly dependent on the aerosol parameters (Figure 2). The scan angle dependence of the phase function also gets weaker (Figure 4). Data from these latitudes are less useful for deriving aerosol parameters from the TOMS data.

Although the single-scattering model is useful for gaining a qualitative understanding of the effects of aerosols on BUV radiances, effects of higher-order scattering at BUV wave-

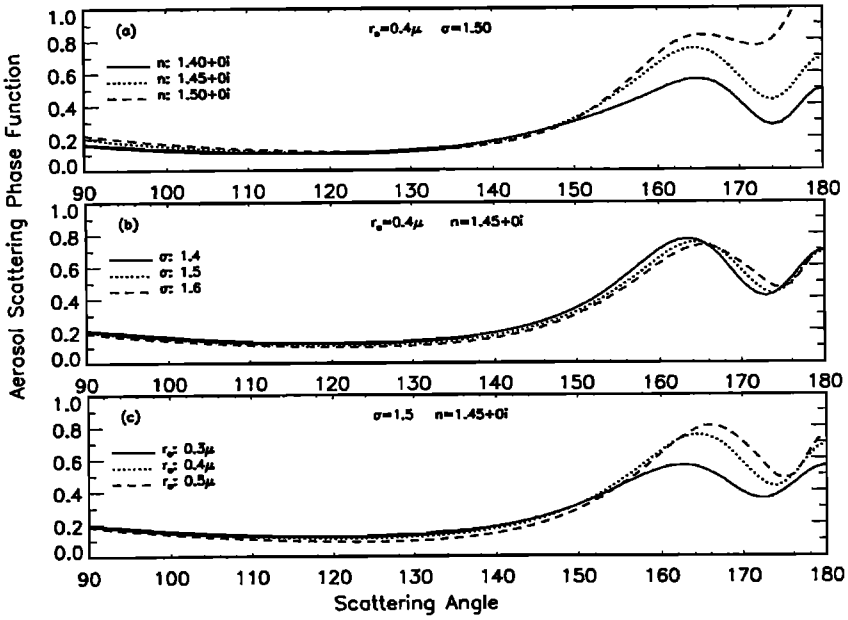

Fig. 2. Sensitivity of aerosol-backscattering phase function at $\lambda = 312.5$ on aerosol parameters. Change in the refractive index (n) produces the largest effect. Effect of changing the width of the lognormal size distribution (σ) is relatively small.

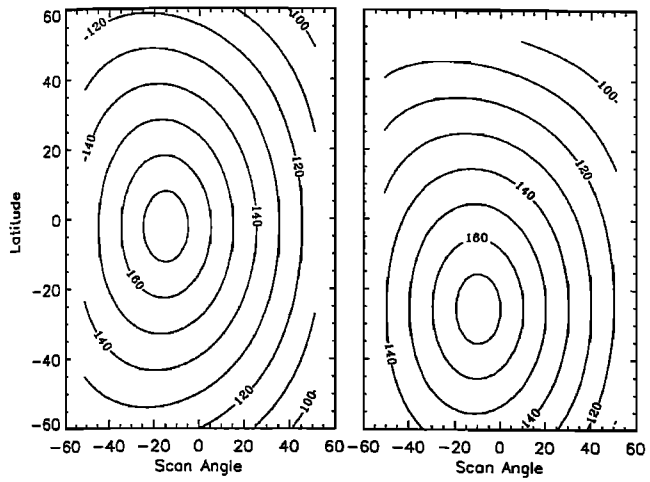

Fig. 3. Scattering angle contours for the total ozone mapping spectrometer (TOMS) instrument on (left) September 21, 1991, and (right) December 21, 1991. 0° scan angle represents the nadir view, positive angles are toward the east of the orbit, and vice versa. The curves are asymmetric around nadir because of the 1100 LT equator crossing time (local time at the subsatellite point) of the Nimbus 7 satellite in late 1991.

lengths are quite large and must be taken into account in modeling the aerosol effect. The radiative transfer program we have used in this study is a modified version of the VPD code developed by *Dave* [1972]. It fully accounts for all orders of scattering, including the effects of polarization. Though the effect of the Earth's sphericity is taken into account for the incoming radiation, higher-order scattering is assumed to take place in a plane parallel atmosphere. Recent calculations (B. Herman, private communication, 1993) using the full spherical geometry suggest that the errors in the modified VPD code are small (<1%) at solar zenith angles less than 80°. In this paper we shall limit our discussion to these solar zenith angles.

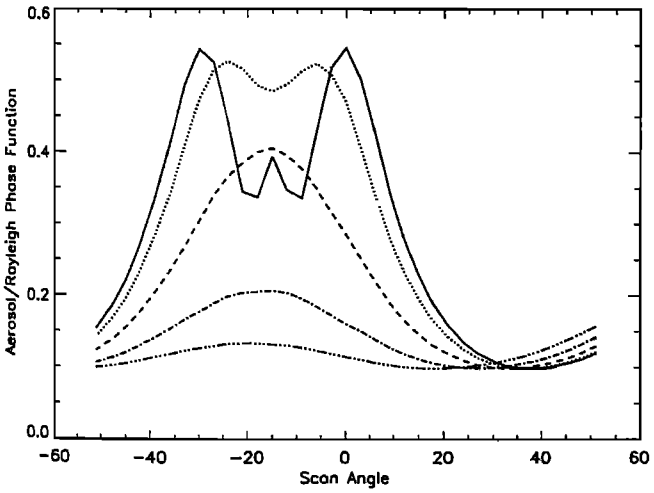

Fig. 4. Ratio of aerosol to Rayleigh-scattering phase function as a function of scan angle for 10° latitude bands centered at 0° (solid curve), 10°N (dotted curve), 20°N, 30°N, and 40°N (dashed curves in decreasing order of magnitude), for September 21, 1991. Southern hemisphere figures would be nearly the same. Phase functions are asymmetric with respect to nadir because the local time of observations is near 1100.

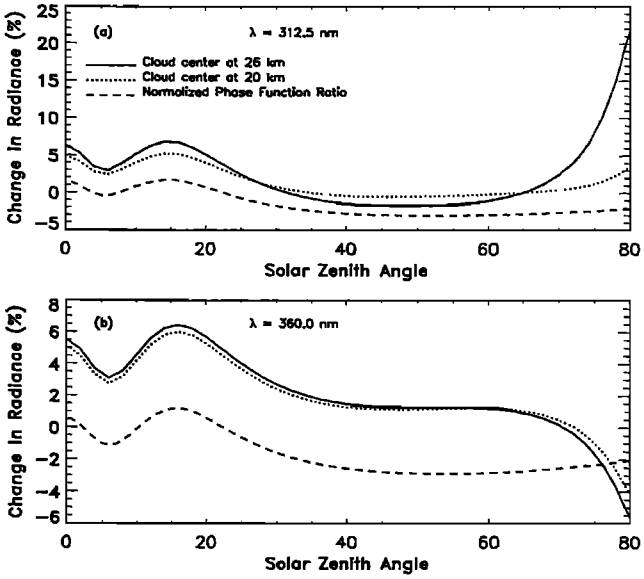

Fig. 5. Percentage increase in nadir-measured backscatter ultraviolet (BUV) radiances as a function of solar zenith angle for aerosol parameters used for Figure 1. Aerosol to Rayleigh phase function ratio (dashed curve) is shown for reference. Aerosols are assumed to have a Gaussian vertical distribution with total optical depth (τ) = 0.20, with peaks at 20 km (dotted curve) and 26 km (solid curve), and σ = 1 km. Low-latitude ozone profile with total column ozone of 275 m atm cm is assumed.

Figure 5 shows the percentage contribution from aerosols to the backscattered radiances in the zenith direction, as seen by the nadir-viewing SBUV series of instruments. At small solar zenith angles, radiance contribution from aerosols is highly correlated with the backscattering phase function. Given the strong forward scattering peak in the aerosol phase function (Figure 1), each scattering by the aerosol particle causes only minor modification in the average direction of the forward beam. Therefore at small solar zenith angles, where multiple scattering within the aerosol layer is relatively small, the primary effect of aerosol scattering is to add singly scattered radiance to the preexisting scattered radiances from the atmosphere. At larger solar zenith angles, when the slant optical path through the aerosols approaches unity, multiple scattering within the aerosol layer strongly enhances the backscattered radiation at the expense of the forward scattered radiation. At non-ozone-absorbing wavelengths, the reduced Rayleigh backscattering from the atmosphere below the aerosol layer is not fully compensated by the aerosol backscattering (for the phase angles being considered), therefore one observes a net reduction of the backscattered radiation. However, at ozone-absorbing wavelengths, high-altitude aerosols may produce a net increase in the backscattered radiation by reducing the absorption by the ozone column below the aerosol layer. This also explains why the aerosol height is so important at the ozone-absorbing 312.5-nm wavelength (Figure 5) but not at 360 nm, where there is negligible ozone absorption. In low latitudes, where the ozone is concentrated in a relatively thin layer near 26 km, the ozone column below a 20-km-high aerosol layer is too small to affect the net ozone absorption. However, at higher latitudes, where the ozone concentration peaks at lower altitudes and is more vertically dispersed, aerosols or thin clouds at even relatively low altitudes can

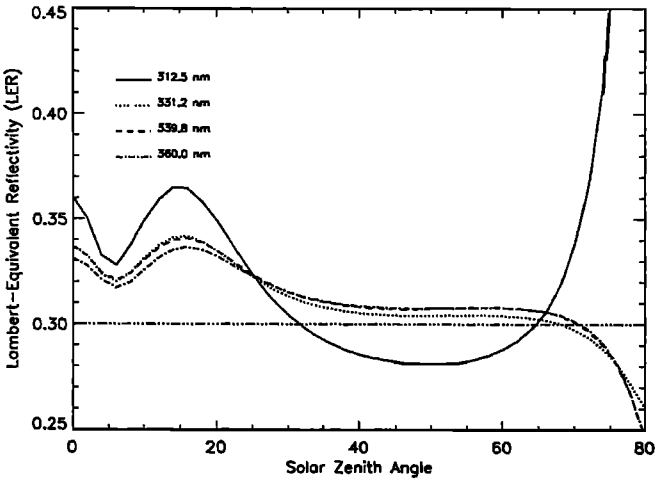

Fig. 6. Lambert-equivalent reflectivity (LER) as a function of solar zenith angle at four BUV wavelengths calculated from aerosol-enhanced radiances for a true surface reflectivity of 0.3 (horizontal line). Aerosol altitude is 26 km, other parameters are same as in Figure 5. Error in BUV-derived total ozone comes from the wavelength dependence of LER.

produce a large effect [*Torres et al.*, 1992]. Therefore one must consider relative peaks of aerosol and ozone vertical profiles to assess the impact of aerosols on BUV radiances.

4. Effect of Aerosols on BUV-Derived Total Ozone Amounts

In the BUV technique, one uses the ratio of radiances measured at a pair of wavelengths, one strongly ozone absorbing and the other weakly absorbing, to determine the total column ozone [*Klenk et al.*, 1982]. Since this ratio depends strongly on surface reflectivity as well as on the ozone amount, a third wavelength, outside the ozone band, is used to estimate the reflectivity. The primary total ozone pair, the *A* pair, is formed by taking the ratio of the radiances at 312.5- and 331.2-nm wavelengths. The *B* pair is formed using 317.5 and 331.2 nm for all instruments except Nimbus 7/TOMS, which uses the ratio of 317.5- and 339.8-nm wavelengths (called *B'* pair). Though the *B'* pair is more sensitive to surface- and cloud-related errors than the *B* pair, it has been used by TOMS to reduce the effects of instrument chopper synchronization problems [*Herman et al.*, 1991]. Also, different BUV instruments have used different wavelengths in the 340- to 380-nm wavelength range to determine the surface reflectivity. In general, the effects of aerosols on derived total ozone are different for different pairs and may depend upon which wavelength is used for deriving the reflectivity. Other observational parameters, such as surface reflectivity, vertical distribution of the aerosol layer, and vertical distribution of ozone are also important. For this paper, however, we will limit our discussion to the basic concepts and consider just a few representative situations. A more detailed report is scheduled for publication as a NASA reference document.

To understand the effect of aerosols on total ozone derived from the BUV experiment, it is useful to consider the concept of Lambert-equivalent reflectivity (LER), first introduced by *Dave* [1977]. In this concept, one replaces the true atmosphere containing clouds and aerosols, bounded by surfaces that are often non-Lambertian, by a purely Rayleigh atmosphere bounded by a fictitious Lambertian surface. LER is the reflectivity of this surface (R), computed by solving the following expression for R:

$$I = I_0 + \frac{RT}{1 - RS_b} \tag{2}$$

where I is the true radiance measured by the satellite, I_0 is the backscatter radiance for a surface of zero reflectivity, T is the once-reflected radiance, and S_b is the atmosphere to surface backscattering. The term in the denominator accounts for multiple reflections from the surface. I_0, T, and S_b are computed from radiative transfer calculations that include all orders of multiple scattering and polarization in a Rayleigh-scattering atmosphere containing varying amounts of ozone [*Dave*, 1964]. The BUV algorithm assumes that the LER thus computed is wavelength independent in the BUV wavelength range (313–380 nm). Otherwise one introduces an error in derived total ozone given by

$$e_\Omega = a(R_1 - R_2) - b(R_1 - R) \tag{3}$$

where R_1 and R_2 are LERs at the pair wavelengths λ_1 and λ_2 and R is the LER at the reflectivity wavelength. Parameters a and b are obtained by radiative transfer calculations and are functions of observational parameters. Typical values of a and b for A pair wavelengths are 3 Dobson units (DU) (1 DU = 10^{-3} m atm cm) and 1 DU, respectively, for a reflectivity difference of 0.01. Radiative transfer calculations show that in the presence of tropospheric aerosols containing no ultraviolet absorbers the calculated LER is very nearly independent of wavelength. Therefore such aerosols produce almost no error in deriving total ozone from the BUV method [*Dave*, 1978].

Figure 6 shows the values of LER for the Mount Pinatubo aerosol, calculated by using (2). Though all LER values show the characteristic aerosol phase function signature, like tropospheric aerosols, they show no wavelength dependence at the weakly ozone-absorbing wavelengths. However, unlike the case of tropospheric aerosols, LER values at 312.5 nm are noticeably different from the other wavelengths. Figure 7 shows the difference in LER for the *A* pair

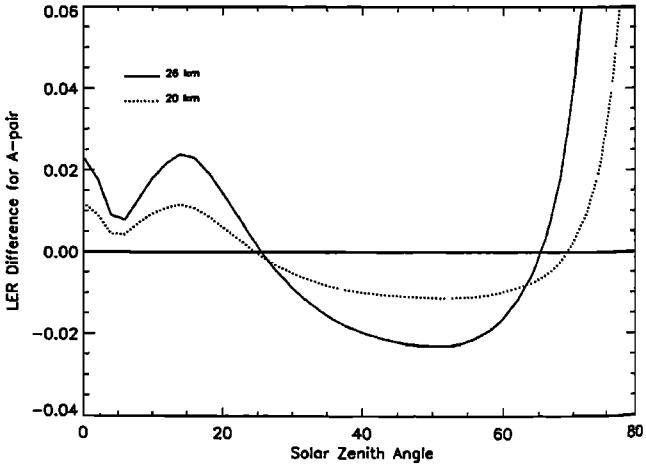

Fig. 7. Difference in Lambert-equivalent reflectivity for the *A* pair wavelengths for aerosols at 26-km (solid curve) and 20-km (dashed curve) altitudes. Aerosol parameters are the same as for Figure 5.

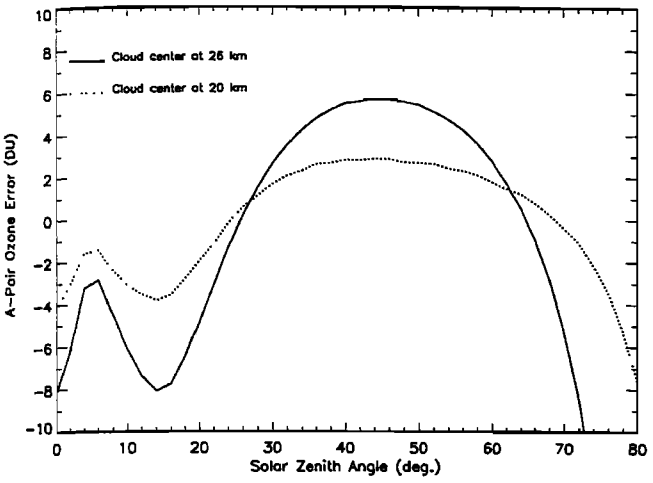

Fig. 8. Error in total ozone derived from the A pair and 340-nm reflectivity as a function of solar zenith angle for a nadir-viewing instrument. Aerosol parameters are the same as for Figure 5.

wavelengths. From (3), one would expect errors in derived total ozone of roughly 3 times the differences in the LERs (the second term in (3) being negligible). Figure 8 shows the ozone error obtained by exact calculation using the operational BUV algorithm.

The reason the 312.5-nm wavelength behaves differently than others is easy to understand. In contrast to the other three wavelengths shown in Figure 6, the 312.5-nm wavelength is strongly absorbed by ozone. Since there is 131 m atm cm of ozone below the assumed 26 km altitude of the aerosol layer, any radiation backscattered by the aerosols would not see this ozone, hence the increase in LER at very low solar zenith angles where the aerosol backscattering phase function is large. At moderate solar zenith angles, where the backscattering phase function is small, effects of aerosol forward scattering dominate, causing increased absorption by the ozone column below the aerosol layer. Finally, at very large angles where the large slant path of the radiation through the aerosol layer is large, backscattering again starts to dominate, causing decreased absorption. Clearly, these effects depend on the amount of ozone column below the aerosol layer, hence the decreased effect of 20-km aerosol; and by inference, one would expect no effect of lower tropospheric aerosols, as seen by *Dave* [1978].

Although the error in BUV-derived total ozone introduced by Mount Pinatubo aerosols is less than 2% (Figure 8) at most solar zenith angles, both the magnitude and the sign of the error vary with solar zenith angle in a way that complicates the analysis of the satellite-derived data when high accuracy is desired. For example, in an extreme case, the ozone error may vary from −8 DU at 15° solar zenith angle to +6 DU at 50° solar zenith angle. These errors would manifest themselves as seasonally varying artifacts in the zonal means. Similar differences would be seen in ozone derived by different satellites that cross a given latitude at different local times.

In the period since the eruption of Mount Pinatubo, six BUV instruments have produced total ozone data. These instruments have flown on satellites that cross the Earth's latitudes at widely different local times. In late 1991 the Nimbus 7 satellite crossed the equator at around 1100 LT, NOAA 11 at around 1500, and the Meteor 3 satellite is in an orbit that precesses with respect to the Sun at the rate of 1.7° per day, which causes the local time of equator crossing to change by 6.8 min per day. Figures 9 and 10 show that these differences in equator crossing times can produce very different error patterns for the three satellites. While the total ozone errors for the NOAA 11/SBUV 2 instrument are always positive in low latitudes (30°S to 30°N), they oscillate between positive and negative values, depending on the season, for the nadir measurements of the Nimbus 7/TOMS

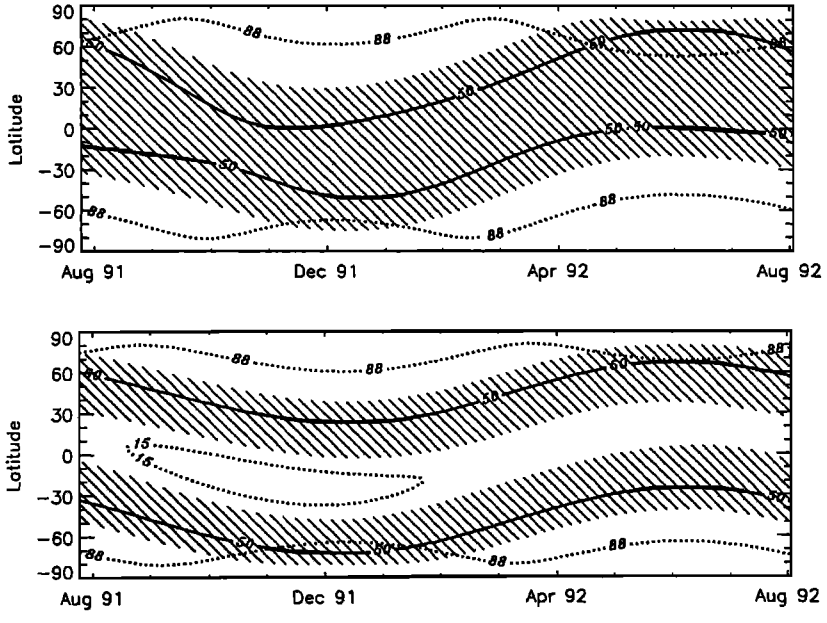

Fig. 9. Shaded areas represent latitudes and times where ozone is overestimated due to aerosols; elsewhere, the ozone is underestimated. Error is maximum positive along the 50° solar zenith angle contour and maximum negative along the 15° contour and near the terminator (88° contour). (Top) For the SBUV 2 instrument on NOAA 11 and (bottom) for the total ozone mapping spectrometer (TOMS) instrument on Nimbus 7 (nadir views only).

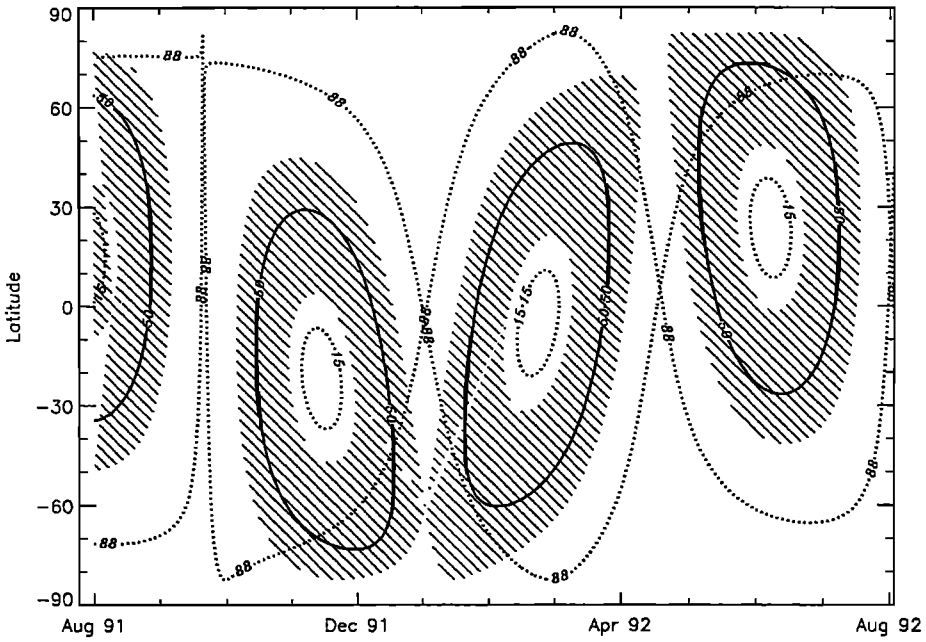

Fig. 10. Same as Figure 9 but for the nadir views of TOMS on the Meteor 3 satellite. Due to the 212-day periodicity of the Meteor 3 orbit, solar zenith angles and hence the error patterns never repeat exactly, as they do for Sun-synchronous satellites.

instrument. For both instruments the ozone is underestimated in middle and high latitudes near the time of winter solstice and overestimated near the time of summer solstice. The magnitude of these errors depends upon the optical thickness and altitude of the aerosol layer. For Meteor 3/TOMS the error patterns (Figure 10) are complicated by the precession of orbit with a period of 212 days. Unlike the Sun-synchronous satellites the solar zenith angles of observations and therefore the error patterns never repeat themselves. Every 106 days (starting October 1, 1991), the satellite goes into a twilight orbit when the solar zenith angle is large at all latitudes. During these times the derived ozone can have large negative errors (Figure 8).

For the two TOMS instruments currently flying, there is the additional complication of changing scattering angle with the scan angle, which causes the errors to vary with the scan angle of the instrument. Exact calculations show that at small solar zenith angles these errors can be determined approximately by using reciprocity, i.e., by replacing the solar zenith angle in Figure 8 with $\pi - \Theta$, where the scattering angle Θ is given by (1). Referring to Figure 3, error is maximum negative along the 165° contour line and maximum positive along the 130° contour line. Because the error changes sign at the 155° scattering angle, errors in the subsolar latitudes oscillate along a scan line: from positive toward the right, negative near the middle, and again positive toward the left. Consequently, the scan average error is much smaller than the maximum error of ±2% at any single position in the scan.

5. Comparison Between Modeled and Observed Errors

With the nadir-viewing SBUV instrument it is difficult to verify the accuracy of aerosol model calculations by direct observation. Because the errors are relatively small and the latitude of observation is highly correlated with solar zenith angle for polar-orbiting satellites, the characteristic signature of aerosol phase function cannot be readily separated from the atmospheric variability of ozone. However, the scanning feature of the TOMS instrument provides a unique capability to directly observe these signatures in the data. The TOMS instrument scans perpendicular to the orbital plane, therefore all the measurements in a given scan are at roughly the same latitude, even though they span a distance of some 2600 km from one end of the scan to the other. Given that the ozone variability over such distances can be quite large, it is necessary to work with zonal means at each scan position rather than with a single scan. Over a week the Nimbus 7 satellite crosses a given latitude about 100 times at many different longitudes. Therefore if one assumes that each of the 35 samples taken along a scan line has randomly sampled the ozone within a given latitude band, in absence of any retrieval errors, the weekly zonal means derived independently from each of the 35 samples should agree to within their statistical uncertainties. Figure 11 shows that prior to the eruption of Mount Pinatubo the agreement between the samples was good, though not perfect (statistical uncertainties are not shown but they are negligible on the scale of the plot). The cause of this small variation has not been established, but small errors in instrument calibration or in spacecraft attitude knowledge could produce such variations. These uncertainties notwithstanding, data taken after the eruption of Mount Pinatubo show a clear and unmistakable signature of aerosol-backscattering phase function (shown in Figure 5) in the scan angle dependence of the zonal mean.

Figure 12 shows a comparison between the observations (corrected for a preexisting scan angle dependent artifact from the previous year) and the modeled errors for various aerosol size distribution parameters. Since the true ozone in the observed data is not known, the modeled errors have

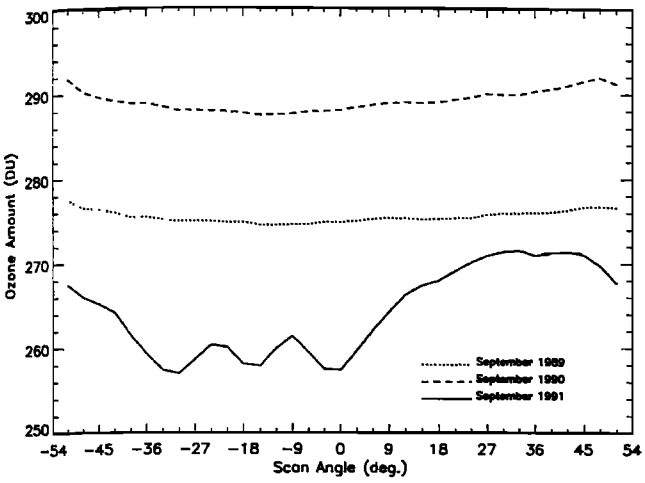

Fig. 11. Scan angle dependence of the zonal mean total ozone derived from TOMS data in the latitude band 5°S to 5°N, in September, for several different years.

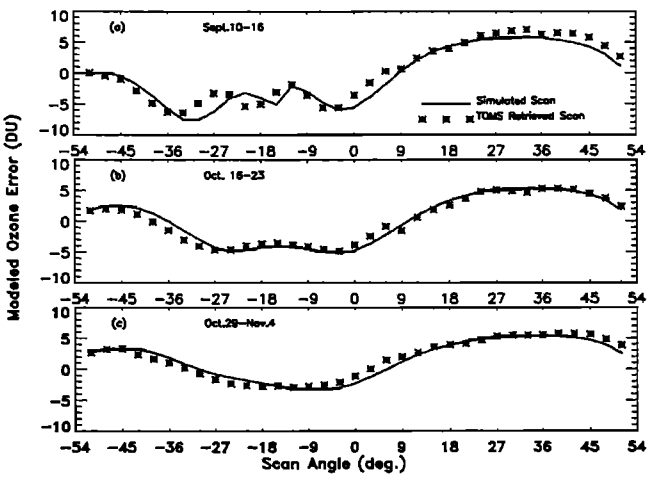

Fig. 13. Comparison between measured and calculated scan angle dependence of ozone derived from the Nimbus 7/TOMS instrument for selected time periods in the latitude band 5°S to 5°N. Aerosol size distribution parameters are same in all figures, but total ozone amount (Ω), aerosol peak altitude z_0, and optical thickness (τ) have been varied to obtain a good fit. Values of these parameters are (*a*) Ω = 263 DU, z_0 = 25.6 km, τ = 0.20; (*b*) Ω = 255 DU, z_0 = 26.2 km, τ = 0.18; and (*c*) Ω = 248 DU, z_0 = 26.2 km, τ = 0.16.

been adjusted to match the observations at the 21° scan angle position, where the model results are insensitive to the aerosol parameters. Agreement between the modeled error and the observed data for the lognormal size distribution parameters, r_0 = 0.4 μm, σ = 1.5, is striking. Figure 13 shows the comparison between the model and the observations for other days and latitude bands. These patterns change dramatically as the scattering angles change with latitude and season, as discussed earlier. During this study, many different combinations of aerosol optical depth, refractive indices, and size distribution parameters were tried, but none provided a match with observations as good as the ones shown. Of course, since there is no practical way to exhaustively search for all possible combinations of these parameters, no claim for uniqueness in deriving these parameters can be made. For example, we have not tried size distributions other than lognormal or distributions with double peaks that might produce a similar scan angle dependence. Nevertheless, our results are in reasonable agreement with in situ measurements of the size distribution parameters [*Valero and Pilewskie*, 1992].

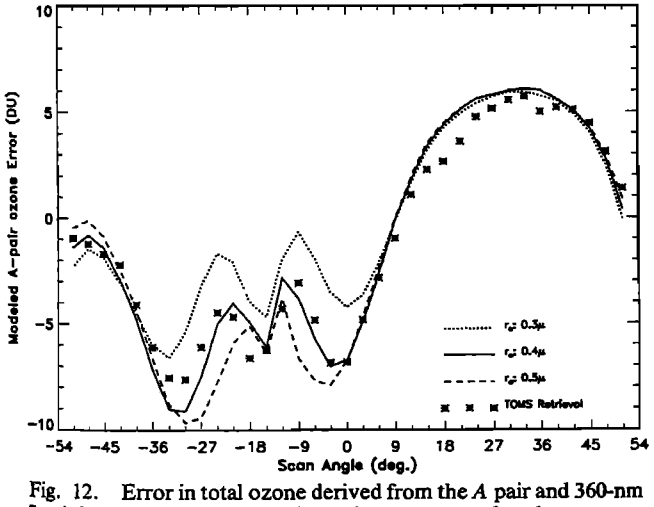

Fig. 12. Error in total ozone derived from the *A* pair and 360-nm reflectivity for the Nimbus 7/TOMS instrument for the average viewing geometry in the latitude band 5°S to 5°N, on September 10–16, 1991, for three selected values of modal radius for a lognormal distribution (width of the distribution (σ) is held constant at 1.5), compared with the zonal mean total ozone derived from the instrument data (symbols). The measured data have been normalized to match the solid curve at the 21° scan angle position, where the error curves are nearly independent of size distribution.

6. CONCLUSION

Radiative transfer calculations show that the aerosol layer in the stratosphere created as a consequence of the eruption of Mount Pinatubo volcano has affected the measurements of total ozone from the BUV family of instruments, several of which are currently operating on NASA, NOAA, and Russian satellites. Total ozone values derived from the cross-track scanning TOMS instrument on the Nimbus 7 satellite show an aerosol-induced artifact as a function of scan angle that agrees well with the modeled errors. Since the modeled scan angle dependence is sensitive to the aerosol parameters, one can infer these parameters by trial and error. The results thus derived agree well with in situ measurements. The agreement between the measured and modeled results give confidence that the effect of aerosols on total ozone derived from BUV instruments is well understood.

At low to moderate solar zenith angles (up to 75°), error in total ozone derived from aerosol-contaminated BUV radiances is of the order of ±2%. However, both the magnitude and the sign of the error are very sensitive to the precise geometry of observation. For the cross-track-scanning Nimbus 7/TOMS instrument the negative and positive errors tend to cancel each other in the zonal mean, giving errors generally less than 1%. Comparison with ground-based Dobson instruments [*Gleason et al.*, 1993] confirm these conclusions. However, at large solar zenith angles (>75%), which occur only in high latitudes near the time of winter solstice (for the Nimbus 7 satellite orbit), the zonal mean ozone from TOMS may be significantly (2–10%) underestimated. The scan angle dependence of the TOMS observations in the subsolar latitudes provides a sensitive tool to

monitor the size distribution parameters of stratospheric aerosols that are difficult to measure from other remote sensing instruments.

REFERENCES

Bhartia, P. K., D. Gordon, K. F. Klenk, C. K. Wong, A. J. Fleig, and D. F. Heath, Observation of El Chichon volcanic aerosols by the solar backscattered ultraviolet (SBUV) experiment, in *Proceedings of the Fifth Conference on Atmospheric Radiation*, American Meteorological Society, Boston, Mass., 1983.

Bluth, G. J. S., S. D. Doiron, C. C. Schnetzler, A. J. Krueger, and L. S. Walter, Global tracking of the SO_2 clouds from the June 1991 Mount Pinatubo eruptions, *Geophys. Res. Lett.*, *19*, 151–154, 1992.

Dave, J. V., Meaning of successive iteration of the auxiliary equation of radiative transfer, *Astrophys. J.*, *140*, 1292–1303, 1964.

Dave, J. V., Development of programs for computing characteristics of ultraviolet radiation, technical report, Vector Case, Int. Bus. Mach. Corp., Fed. Syst. Div., Gaithersburg, Maryland, 1972.

Dave, J. V., Investigation of the effect of atmospheric dust on the determination of total ozone from the earth's ultraviolet reflectivity measurements, *NTIS-N77-24690–24692*, Natl. Tech. Inf. Serv., Springfield, Va., 1977.

Dave, J. V., Effect of aerosols on the estimation of total ozone in an atmospheric column from the measurements of its ultraviolet radiance, *J. Atmos. Sci.*, *35*, 899–911, 1978.

Gleason, J. F., et al., Record low global ozone in 1992, *Science*, *260*, 523–526, 1993.

Herman, J. R., R. Hudson, R. McPeters, R. Stolarski, Z. Ahmad, X. Y. Gu, S. Taylor, and C. Wellemeyer, A new self-calibration method applied to TOMS and SBUV backscattered ultraviolet data to determine long-term global ozone changes, *J. Geophys. Res.*, *96*, 7531–7545, 1991.

Hofmann, D. J., and J. M. Rosen, Stratospheric sulfuric acid fraction and mass estimate for the 1982 volcanic eruption of El Chichon, *Geophys. Res. Lett.*, *10*, 313–316, 1983.

Klenk, K. F., P. K. Bhartia, A. J. Fleig, V. G. Kaveeshwar, R. D. McPeters, and P. M. Smith, Total ozone determination from the Backscattered Ultraviolet (BUV) experiment, *J. Appl. Meteorol.*, *21*, 1672–1684, 1982.

McCormick, M. P., and R. E. Veiga, SAGE II measurements of early Pinatubo aerosols, *Geophys. Res. Lett.*, *19*, 155–158, 1992.

Palmer, K. F., and D. Williams, Optical constants of sulfuric acid: Application to the clouds of Venus, *Appl. Opt.*, *14*, 208–219, 1975.

Schoeberl, M. R., P. K. Bhartia, E. Hilsenrath, and O. Torres, Tropical ozone loss following the eruption of Mt. Pinatubo, *Geophys. Res. Lett.*, *20*, 29–32, 1993.

Torres, O., Z. Ahmad, and J. R. Herman, Optical effects of Polar Stratospheric Clouds on the retrieval of TOMS total ozone, *J. Geophys. Res.*, *97*, 13,015–13,024, 1992.

Valero, F. P. J., and P. Pilewskie, Latitudinal survey of spectral optical depths of the Pinatubo volcanic cloud-derived particle sizes, columnar mass loadings, and effects on planetary albedo, *Geophys. Res. Lett.*, *19*, 163–166, 1992.

P. K. Bhartia, J. Herman, and R. D. McPeters, NASA Goddard Space Flight Center, Mail Code 916, Greenbelt, MD 20771.

O. Torres, Hughes STX Corporation, 4400 Forbes Boulevard, Lanham, MD 20706.

(Received April 9, 1993;
revised June 18, 1993;
accepted June 20, 1993.)